Hindawi
Mobile Information Systems
Volume 2022, Article ID 1898066, 11 pages
https://doi.org/10.1155/2022/1898066

Research Article

Research on the Application of Computer-Assisted Translation Technology in Translation Teaching

Yang Yang and Meng Su

North China Institute of Aerospace Engineering, Lang Fang 065000, China

Correspondence should be addressed to Yang Yang; wywl0110@nciae.edu.cn

Received 5 July 2022; Revised 22 August 2022; Accepted 26 August 2022; Published 15 September 2022

Academic Editor: Jiafu Su

In order to improve the quality of translation teaching, this study combines computer-aided translation technology to construct a translation teaching system, uses digital signal processing as a technical means to process waveform data online, and designs digital models for signal flow. Moreover, this study designs a digital filter to suppress waveform noise to improve the accuracy of amplitude measurement and uses a hardware algorithm for accumulating shift and averaging to correct the baseline stacking effect in real time. In addition, this study builds an intelligent translation software system with the support of algorithms in combination with translation requirements and conducts experimental verification of translation digital processing. Finally, the simulation experiment verifies the digital translation processing effect of the method in this study, and the application effect of computer-aided translation technology in translation teaching is verified through teaching evaluation research.

1. Introduction

The continuous progress of society and the increasing frequency of international exchanges have expanded the demand for compound translators in the international market. At present, many domestic colleges and universities have opened English majors, and even some colleges and universities have opened translation majors at the undergraduate level. However, although thousands of graduates pour into the market every year, they still cannot meet the needs of the society for translation talents. The main reason for this phenomenon is that the students' translation practice ability fails to meet the requirements of the translation market. The translation teaching mode of school teachers directly affects students' translation practice ability. The traditional "teacher-centered, text-based" translation teaching mode largely limits the cultivation of students' translation application ability. However, the continuous updating of computer information technology has promoted the innovation of translation methods and translation tools. Moreover, computer-aided translation (CAT) has become a necessary application technology for translation agencies.

Translation teaching has always followed the teaching of language skills from the bottom up. Traditional translation teaching takes teachers as the center, ignores the subject status of students, and cannot effectively cultivate students' translation practice ability and creativity. Translation teaching should change from "teacher-centered to student-centered" [1], in order to change the drawbacks brought by traditional translation teaching. The focus of the American interactive language teaching method is to take students as the center. According to the individual characteristics of students and the differences in teaching resources, teachers adopt diversified and flexible teaching methods according to their own teaching characteristics, so as to avoid students' passive learning state [2]]. The application of the interactive language learning method in translation teaching helps students to have a deep understanding of translation theories and techniques. In the mode of translation workshops, it is more conducive to creating a learning atmosphere of interaction between teachers and students. The learning exchange between students can cultivate students' autonomous learning ability, especially eliminate the tension of students in traditional classrooms, and then better participate in various teaching links designed by teachers [3]. In the computer-aided translation (CAT) environment, the process of simulating professional translation in the classroom can be realized, and the combination with the workshop style translation environment can truly build a professional translation ability training for students and collaborative ability development for the purpose. On the other hand, by supervising the translation process, teachers can monitor and summarize students' errors in the translation process, and provide a wide range of teaching data bases for teachers' translation teaching, which is conducive to teachers' design of personalized lesson plans, so as to better carry out translation teaching [4].

Compared with the traditional teaching concept of one-sided strengthening of social values, CAT translation teaching pays more attention to the individual development of students. In the era of "a hundred flowers blooming", it is undoubtedly better to cultivate talents with flamboyant personality, and education has achieved the purpose of "not only making people learn to do things (todo), but more importantly, making people learn to be people (tobe)" [5]. In this sense, the research on the training mode of translation talents under CAT translation teaching starts from the students, and the end point is also on the students. Only by fully understanding the needs of students, learning needs initiated by students to promote teaching reform, and changing top-level design to guide school-based design to school-based design to promote top-level design, this model is the focus of our research [6].

Translation teaching in colleges and universities is a special education category that integrates the characteristics of vocational education and higher education. On the one hand, translation teaching in colleges and universities should aim at cultivating practical translation talents [7]. However, translation teaching is only a subject teaching under the English major, and the teaching time is limited, only a short one year. Therefore, it is impossible to organize the teaching content according to the logical sequence of subject knowledge, emphasizing the comprehensiveness, system, and depth of the curriculum. Only if the curriculum structure is reasonable, the main body (students) of translation teaching can not only learn something in just one year but also lay the foundation for future personal development. The content of CAT translation teaching integrates computer skills, translation tools application, translation skills training, and other aspects of knowledge. The deeper content is that students can improve themselves and form their own values, professional ethics, and social responsibility through the self-construction of this knowledge and abilities [8]. Then, how to structure the CAT translation course is the core. Xu Bin proposed that in the CAT teaching system, the following teaching modules should be reasonably adjusted (but must be included): (1) the translation information technology module, including advanced word processing skills, digital text acquisition technology, input technology, search technology, corpus; (2) terminology work, that is, the establishment and management of termbase (TM) [9]; (3) CAT system application (such as SDL Trados, D6jaVu, Yaxin, etc.); and (4) translation project management, that is, familiarity with translation normal work of the company. These CAT teaching modules should be said to be very specific. These modules cover most of the content in CAT teaching and lay a solid foundation for students to move towards professional translation in the future. At the same time, the content of CAT practice also tends to be translated (for example, tenders, contracts, annual reports, etc., the content of the same field is highly overlapping), which fully shows that CAT teaching is an atypical professional teaching. But as mentioned above, translation teaching in colleges and universities is a special education category that combines the characteristics of vocational education and higher education [10]. "The teaching of translation can be divided into three levels: first, teaching translation as a purely foreign language teaching method; second, translation teaching as a foreign language professional course; third, translation professional teaching as a translation professional course." They further clearly pointed out: "First The third level belongs to the teaching translation, the purpose is to improve the foreign language level; the third level belongs to the translation teaching, the purpose is to cultivate professional translators; The primary course for translation talents [11]." In this sense, the teaching trend of CAT professionalization has weakened the meaning contained in the "advanced course of foreign language teaching" to a certain extent, that is, translation in the traditional "literary translation". Theoretical study and the cultivation of humanistic quality. CAT teaching weakens theoretical teaching (but also includes theoretical learning) and emphasizes applied translation practice (and occasionally literary translation) [12]. Therefore, how to resolve the contradiction between the two is also an important part of the curriculum. There are two solutions: one is to arrange a certain time (for example, 1/3 of one year's translation teaching time) to specially arrange to explain the theoretical part and do literary translation practice; the other is to use the MT (It consciously asks students to do bilingual parallel corpus (memory bank) of literary translation, and then through the query and comparison of corpus, analysis and explanation, the theoretical learning part and the practical content of literary translation are evenly distributed in the whole translation teaching activities. From the practical effect, the second method seems to be easier for students to accept [13]. Therefore, in addition to the four teaching modules mentioned by Xu Bin, the CAT teaching system should add a "translation appreciation and evaluation". This module focuses on the appreciation and evaluation of literary translation. In the appreciation and evaluation, it explains translation theory, experiences translation skills, and accepts humanistic influence [14].

Considering the class hours and task volume of translation courses, traditional translation courses are basically evaluated by a test study at the end of the semester. This summative evaluation method results in a single evaluation content, evaluation subject, and evaluation link, and it is difficult to achieve the evaluation effect [15]. The translation teaching of CAT should change this summative evaluation into a formative evaluation. The five major modules in the CAT teaching system are both independent and intersecting, especially the four modules mentioned by Xu Bin, if one is not learned, it will affect the learning effect of the entire CAT. For example, if you do not know "advanced word processing", you cannot import the CAT system (such as trados) normally when dealing with some manuscripts with messy formats such as Word documents. Even if you import people, many tags will be displayed in the CAT system, causing translation time trouble. For another example, if you do not create, maintain, and edit a memory library (MT) or term library (TM), you will not be able to fully and effectively utilize the functions of the CAT system, and will not achieve the purpose of saving time and efficiency. Therefore, CAT teaching is an interlocking teaching activity, which also automatically makes the traditional summative assessment evolve into a formative assessment [16].

This study combines computer-aided translation technology to construct a translation teaching system, improve the quality of translation teaching in colleges and universities, and promote the intelligent development of translation teaching.

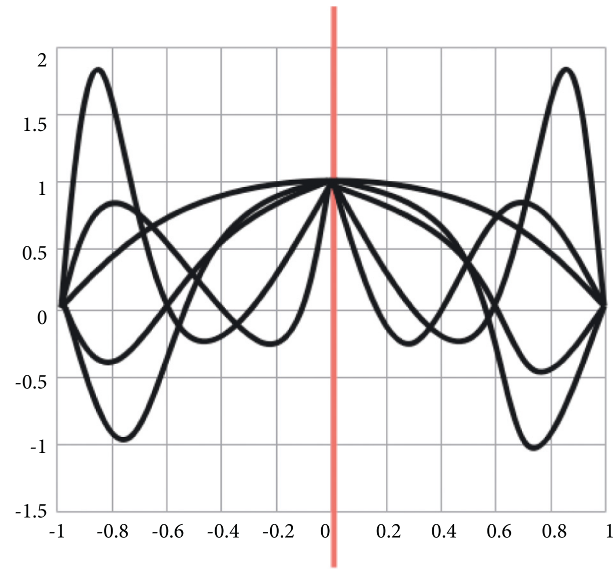

Figure 1: :Runge phenomenon.

2. Digital Processing of Translation Signals

2.1. DSP Digital Signal Processing. The main idea of digital Constant Fraction Timing (dCDT) is that after the nuclear pulse waveform is input, the ADC obtains accurate waveform amplitude information and collects enough waveform front-end points. By combining "coarse" counting and "fine" measurement, "coarse" counting is implemented by the FPGA high-order counter, which achieves a time resolution of 8 ns of ADC sampling time. Furthermore, "fine" measurements rely on DSP for waveform interpolation, which is reconstructed within one clock cycle. Its timing accuracy can be much smaller than the ADC clock period, reaching sub-nanosecond (100~10 ps) time resolution.

The AD9445 samples the entire waveform. The data enter the FPGA and undergoes FIR filtering and baseline recovery. After processing, the data is sent to the DSP, and the assembly function is used to send minidx (falling edge)/ maxidx (rising edge) to find the peak value in the data sequence. Although the more sampling points during the fitting, the more accurate the fitting accuracy is, at the same time the fitting time is also longer, resulting in an excessively long dead time window for DSP processing. Then, we select one sample point on the left side of the peak and two sample points on the right side, and we do a polynomial interpolation fit with a total of 4 points.

In scientific experiments or statistics, people often need to obtain an approximate expression $y = (x)$ for the independent variable x and the dependent variable y from a set of measured discrete data points (x, y). $i = 0.1, \ldots, n$. This is to construct a mathematical approximation function $\varphi(x)$ from a given N points $(x. y)$, which requires the $\varphi(x)$ function curve to pass through all given points $(x.y)$ with equal function values, then $\varphi(x)$ is called an interpolation function.

The commonly used interpolation methods can be divided into two categories: algebraic polynomial interpolation and piecewise interpolation. For example, Lagrange interpolation and Newton interpolation belong to polynomial interpolation, and cubic spline interpolation belongs to piecewise interpolation. The advantage of algebraic polynomial interpolation is that the format is neat and standardized, but the disadvantage is that the Runge phenomenon will appear in high-order polynomials. As shown in Figure 1, the interpolation polynomial oscillates violently in the interpolation interval;

The Nth degree algebraic interpolation polynomial is:

$P_n(x) = a_0 + a_1 x + \ldots + a_n x^n$ is an Nth algebraic interpolation polynomial, and the function is determined by $(n+1)$ coefficients $a_0, a_1, \ldots, a_n$:

When the curve passes through $(n+1)$ mutually different interpolation points (x_i, y_i) in a given plane, a linear system of equations can be obtained:

$$\begin{cases} a_0 + a_1 x_0 + a_2 x_0^2 + \ldots + a_n x_0^n = y_0, \\ a_0 + a_1 x_1 + a_2 x_1^2 + \ldots + a_n x_1^n = y_1, \\ \cdots \\ a_0 + a_1 x_n + a_2 x_n^2 + \ldots + a_n x_n^n = y_n. \end{cases} \quad (1)$$

The coefficient determinant of the system of (1) is the Vandermonde determinant:

$$V(x_0, x_1, \ldots, x_n) = \begin{vmatrix} 1 & x_0 & x_0^2 & \ldots & x_0^n \\ 1 & x_1 & x_1^2 & \ldots & x_1^n \\ \ldots & & & & \\ 1 & x_n & x_n^2 & \ldots & x_n^n \end{vmatrix}. \quad (2)$$

When x_i are different from each other, there is $\prod_{0 \le j \le i \le n} (x_i - x_j) \neq 0$, and the solution of the system of equations exists and is unique.

For $n+1$ different interpolation nodes (x, y), $i = 0, 1, \ldots, n$, based on the uniqueness of the Nth interpolation polynomial, a corresponding nth interpolation basis function 1

(x), $i-0,1, \ldots, n$ can be defined for each interpolation node x_i:

It is required that $x_0, x_1, \ldots, x_{i-1}, x_i, \ldots, x_n$ is the zero point of 1. (x), which can be set as:

$$l_i(x) = a_i(x-x_0)(x-x_1)\ldots(x-x_{i-1})(x-x_{i+1})(x-x_n), \tag{3}$$

$l_i(x_i) = 1, x = x_i$ is brought into the above formula to get:

$$l_i(x_i) = a_i(x_i-x_0)(x_i-x_1)\ldots(x_i-x_{i-1})(x_i-x_{i+1})\ldots(x_i-x_n) = 1$$

$$l_i(x) = \frac{(x-x_0)(x-x_1)\ldots(x-x_{i-1})(x-x_{i+1})\ldots(x-x_n)}{(x_i-x_0)(x_i-x_1)\ldots(x_i-x_{i-1})(x_i-x_{i+1})\ldots(x_i-x_n)} = \prod_{\substack{0\le j\le n\\ j\ne i}} \frac{x-x_j}{x_i-x_j} \tag{4}$$

The combined basis function is:

$$L_n(x) = \sum_{i=0}^{n} l_i(x) y_i. \tag{5}$$

That is, the Nth order Lagrangian interpolation polynomial.

Among them, linear interpolation is the simplest form of polynomial interpolation, and cubic Lagrangian interpolation polynomial is also called cubic interpolation.

$$L_n = \sum_{i=0}^{n} l_i(x) f(x_i) l_i(x) = \prod_{\substack{0\le j\le n\\ j\ne i}} \frac{x-x_j}{x_i-x_j} \quad n = 3. \tag{6}$$

Piecewise interpolation is to divide the sequence (x_i, y_i) into segments. Only the discrete points in the small interval are fitted with the interpolation function, and each small interval is connected again to obtain the overall interpolation fitting. The advantage is that the local properties are good, and the disadvantage is that the interpolation nodes are not smooth.

The cubic spline interpolation polynomial is also called Spline interpolation: it is to construct a cubic polynomial in each sub-interval $[x_i, x_{i+1}]$, the function has equal function values at the nodes, and the first and second derivatives are required to be continuous. Each interval spline function can be uniquely determined by boundary conditions. The main advantage is that the degree of smoothness is high, and the parameters need to be solved by the undetermined coefficient method of the equation system, and the workload is larger than that of the polynomial interpolation method.

Cubic spline interpolation function $S(x)$: for $n+1$ nodes $[x_i, y_i], i = 0, 1, \ldots, n$ on a given interval $[a, b]$, the function $S(x)$ satisfies $S(x_i) = y_i$. $S(x)$ is at most a cubic polynomial on each cell interval $[x_i, x_{i+1}]$, and $S(x)$ has continuous second-order derivatives on $[a, b]$;

The existence and uniqueness of the constructed spline function can be determined by the method of undetermined coefficients.

Mark $M_i = S''(x_i), m_i = S'(x_i), i = 0, 1, \ldots, n$ is defined. Since $S''(x_i)$ is a linear function on the sub-interval $[x_i, x_{i+1}]$, a piecewise linear interpolation function of M is performed on $[x_i, x_{i+1}]$:

$$S''(x) = \frac{x-x_{i+1}}{x_i-x_{i+1}} M_i + \frac{x-x_i}{x_{i+1}-x_i} M_{i+1}, i = 0, 1, \ldots, n. \tag{7}$$

We set $h_i = x_{i+1} - x_i$ to get:

$$S''(x) = \frac{x_{i+1}-x_i}{h_i} M_i + \frac{x-x_i}{h_i} M_{i+1}, i = 0, 1, \ldots, n. \tag{8}$$

$S''(x)$ is integrated twice to get:

$$\begin{aligned} S(x) &= \frac{(x_{i+1}-x)^3}{6h_i} M_i + \frac{(x-x_i)^3}{6h_i} M_{i+1} + cx + d, \\ &= \frac{(x_{i+1}-x)^3}{6h_i} M_i + \frac{(x-x_i)^3}{6h_i} M_{i+1} \\ &\quad + C(x_{i+1}-x) + D(x-x_i) \end{aligned} \tag{9}$$

$S(x_i) = y_i, S(x_{i+1}) = y_{i+1}$ is substituted into the above formula, it can be solved:

$$C = \frac{y_i}{h_i} - \frac{h_i M_i}{6}, D = \frac{y_{i+1}}{h_i} - \frac{h_i M_{i+1}}{6}. \tag{10}$$

Therefore, on $[x_i, x_{i+1}]$, there is

$$S(x) = \frac{(x_{i+1}-x)^3 M_i + (x-x_i)^3 M_{i+1}}{6h_i} + \frac{(x_{i+1}-x) y_i + (x-x_i) y_{i+1}}{h_i} - \frac{h_i}{6}\left[(x_{i+1}-x) M_i + (x+x_i) M_{i+1}\right] x \in (x_i, x_{i+1}), \quad i = 0, 1, \ldots, n. \tag{11}$$

By $S_i'(x_i) = S_{i-1}'(x_i)$, the system of equations can be obtained:

$$\begin{gathered}\mu_i M_{i-1} + 2M_i + \lambda_i M_{i+1} = d_i, i = 0, 1, \ldots, n \\ \lambda_i = \frac{h_i}{h_i + h_{i+1}}.\end{gathered} \tag{12}$$

Among them, there is $\mu_i = 1 - \lambda_i d_i = (6/(h_i + h_{i+1}))((y_{i+1} - y_i/h_i) - (y_i - y_{i-1}/h_{i-1})) = 6y(x_{i-1}, x_i, x_{i+1})$

When the values of M and M are given (when there is $M = 0$, $M. = 0$, it is called the natural boundary condition), at this time, the $n-1$ order equation system has n-1 unknowns, $i = 0, 1, \ldots, -1$, that is:

$$\begin{bmatrix} 2 & \lambda_1 & & \\ \mu_2 & 2 & \lambda_2 & \\ \cdots & \cdots & \cdots & \\ \mu_{n-2} & 2 & \lambda_{n-2} & \\ \mu_{n-1} & 2 & & \end{bmatrix}\begin{bmatrix} M_1 \\ M_2 \\ \cdots \\ M_{n-2} \\ M_{n-1}\end{bmatrix} = \begin{bmatrix} d_1 - \mu_1 M_0 \\ d_2 \\ \cdots \\ d_{n-2} \\ d_{n-1} - \lambda_{n-1} M_n \end{bmatrix}. \tag{13}$$

The tridiagonal band matrix of the above (8) is solved, and the spline interpolation function of the discrete data system can be constructed. In the actual DSP time interpolation, linear interpolation, cubic interpolation, and spline interpolation are programmed through Matlab simulation. At the same time, it is tested in the DSP environment. In terms of interpolation accuracy, spline interpolation is the best, and in terms of execution speed, linear interpolation is the best. However, the DSP computing load and computing accuracy are considered comprehensively. From the real-time consideration, we use cubic interpolation to do our time interpolation function.

Through the cubic waveform interpolation expression obtained above, we construct the peak function curve from the 4-peak data given by the waveform peak finding function. Mathematically, to find the extreme value of the function, the numerical method — the chord tangent method is usually used, as shown in Figure 2.

If the first derivative of the peak function $L_z(x)$ is assumed to be $f(x)$, that is:

$$L_3'(x) = f(x). \tag{14}$$

Then, the root of $f(x)$ is the extremum of the function. The tangent method formula is defined as follows:

$$x_{k+1} = x_k = \frac{f(x_k)}{f'(x_k)} = x_k - \frac{f(x_k)(x_k - x_{k-1})}{f(x_k) - f(x_{k-1})}. \tag{15}$$

That is, the difference quotient is used to replace the derivative operation, and $f'(x_k) = \Delta f(x)/\Delta x = f(x_k) - f(x_{k-1})/x_k - x_{k-1}$.

The tangent method requires that two initial points x_0, x_1 are given at the beginning, and then $x_2, \ldots$ are obtained according to x_0, x_1. According to x_k、 x_k, x_{k+1} is obtained, and loop approximation is performed until the interpolated value of x obtained twice is $\leq \varepsilon$. We consider that approximate numerical roots are found.

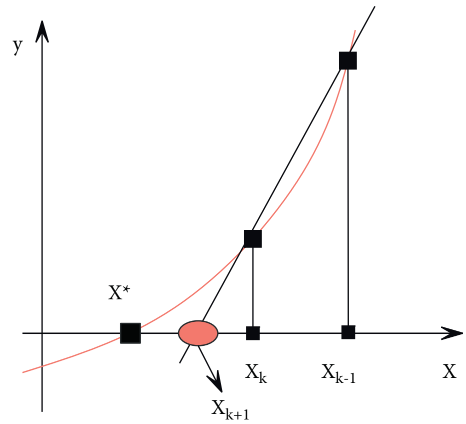

Figure 2: Chord tangent method to find function roots.

If it is assumed that the minimum value of the function is to be found, and x is known to be the minimum value of the sequence, then the extreme position of the function falls within the interval $[x_0, x_1]$ or $[x_1, x_2]$. First, the initial interval is given, and then the midpoint value of the interval is taken and substituted into the formula to calculate the midpoint function value y_m. Compared with the initial interval, the larger half interval is discarded, and the bisection approximation is recirculated until $y \leq \varepsilon$ is obtained twice, and the approximate value is considered to be obtained.

The extreme value is obtained by the peak interpolation curve, and the interpolation amplitude $S_{amplitu\,de}$ of the waveform only needs to be multiplied by the constant ratio factor p. The reading value that fluctuates with the fluctuation of the waveform amplitude is obtained: $S_{threshold} = p * S_{amplitude}$

2.2. ADC Linearity Test. ADC is the key performance factor of the timing measurement system. ADC has many test indicators. What we care about is the overall linearity test indicator of the analog part of the system including ADC acquisition and op amp filtering.

The ADC integral nonlinearity (INL) is the deviation of the actual conversion curve from the ideal conversion curve, as shown in Figure 3:

$$INL = \frac{V_D - V_{zero}}{V_{LSB\_ideal}} - D, 0 < D < 2^N - 1. \tag{16}$$

The principle of the integral nonlinear static test is as follows: a single channel is an input with a certain DC voltage Vs, and the corresponding amplitude value measured by the ADC is recorded. According to the test data, the ADC static conversion curve of the channel is fitted by Matlab software. The drive AD8139 used in the dCFT system is inverting amplification, and in the ^{22}Na positron experimental test platform, a gain of 2 input signals for the driver circuit is required to obtain the optimal input amplitude. The static integral nonlinearity of dCFT platform channel A is shown in Figure 4, and the static integral nonlinearity of dCFT platform channel A is shown in Figure 5.

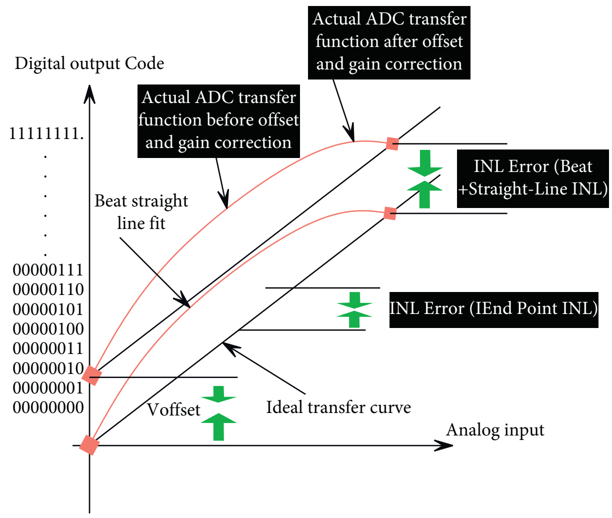

FIGURE 3: Schematic diagram of integral nonlinear.

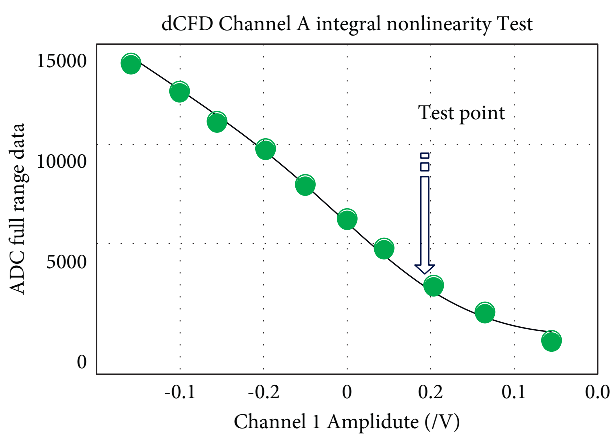

FIGURE 4: Static integral nonlinearity of dCFT channel A.

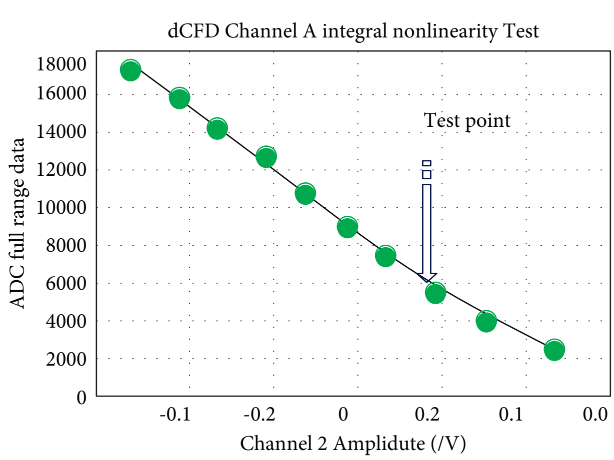

FIGURE 5: Static integral nonlinearity of dCFT channel B.

Differential nonlinearity (DNLA) is the relative deviation between the code width and the ideal code width in the actual conversion characteristics of the analog-to-digital conversion circuit, as shown in Figure 6.

$$DNL = \frac{V_{D+1} - V_D}{V_{LSB\_ideal}}, 0 < D < 2^N - 1. \tag{17}$$

The differential nonlinear dynamic test principle is as follows: a single channel is applied with a continuous analog signal, and the sampling output code is statistically analyzed to obtain the test circuit performance parameters, which is called the code density histogram test method. According to the difference in the added analog signal, it is divided into the ramp method (Ramp) and the sine method (Sine). The ADC samples a period of signal input, and the number of occurrences of different code outputs is called the code density. The ADC's output codes and their occurrences are plotted as coordinates, and the resulting graph is a code density histogram. In the histogram, each code is called a bin, and the number of occurrences of each code is called the bin width. The nonlinear parameters of the ADC can be calculated from the code density data.

The code density histogram test requirements are:

(1) Test data sampling data volume requirements

The code density histogram method is utilized to measure the dynamic performance of the ADC circuit, which is based on statistical theory. Therefore, in order to ensure the reliability and accuracy of the test, the data sample is required to be large enough. It can be obtained from the statistical theoretical analysis that the reliability (Z) and error (B) of the analysis method and the required number of samples and the number of ADC bits (N) have the following relationship:

$$N_{\text{Record}} = \frac{\pi \times 2^{N-1} \times (Z)^2}{\beta}. \tag{18}$$

For example, the number of ADC bits is 10Bit, the DNL and INL errors are required to be controlled within 0.1 LSB, and the analysis reliability is 95%. At the same time, the actual required sample data volume is $N_{\text{Resond}} = 617{,}920$, the analysis reliability is 99%, and the actual required sample data volume is $N_{\text{kscord}} = 1{,}070{,}678$. Moreover, the number of ADC bits is 14 Bit, the DNL and INL errors are required to be controlled within 0.1 LSB, and the analysis reliability is 95%. The actual required sample data volume is $N_{\text{Reced}} = 9{,}886{,}720$, the analysis reliability is 99%, and the actual required sample data volume is $N_{\text{Recowd}} = 17{,}130{,}848$;

(2) The sampling frequency and the sine wave input frequency cannot be correlated

The basis of the code density histogram measurement is to randomly sample the input signal, that is, to select an appropriate sampling frequency and signal frequency to ensure that the sampling circuit does not always repeatedly sample the same level. That is, the sampling frequency and the signal frequency are not allowed to have an integer multiple relationship, so as to ensure that the two are not related. In addition, the time jitter, reference drift,

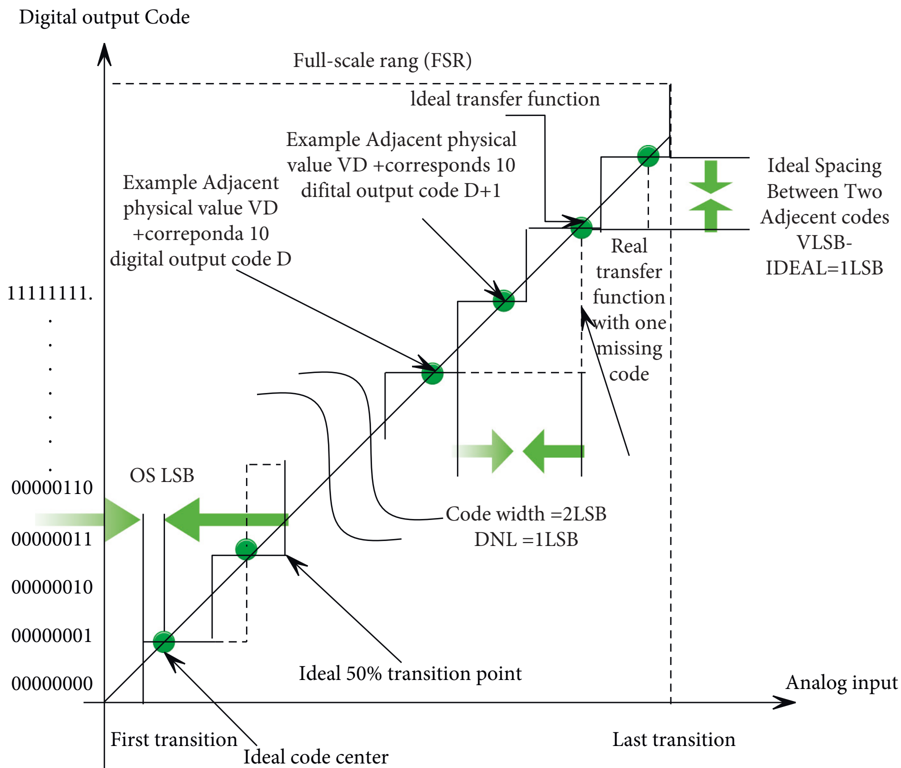

Figure 6: Schematic diagram of differential row linearity.

and frequency drift in the actual ADC circuit will make the sampling process more random.

(3) Selection of test signal

Usually, the code density test method often uses a ramp signal (triangular wave or sawtooth wave) or a sine signal as the input signal. The waveform code density histogram of the ramp method is ideal. Except for the two symbols at the edge, the number of output symbols is the same. However, the biggest problem is that when the frequency of the required input signal is high and the accuracy of the ADC circuit under test is high, it is difficult to obtain an input signal that meets the test requirements, and the nonlinearity and distortion of the input signal will have a greater impact on the test results.

For high-speed ADC circuit testing, a sine wave signal is usually used as the input signal. On the one hand, a sine wave can be obtained by filtering and other means to obtain a relatively ideal waveform. On the other hand, a sine wave can be precisely defined mathematically, and noise and dynamic distortion can be easily analyzed in the frequency domain. The ideal code density histogram of the sine wave is shown in Figure 7, and the actual discrete sampling code box histogram is shown in Figure 8.

The sine wave input signal is set to V_i, and there is $V_{IN} = A\sin(\omega t)$, we set $g(t) = A\sin(\omega t)$. Then, t can be regarded as a random variable, and within 0-T, t is uniformly distributed, that is:

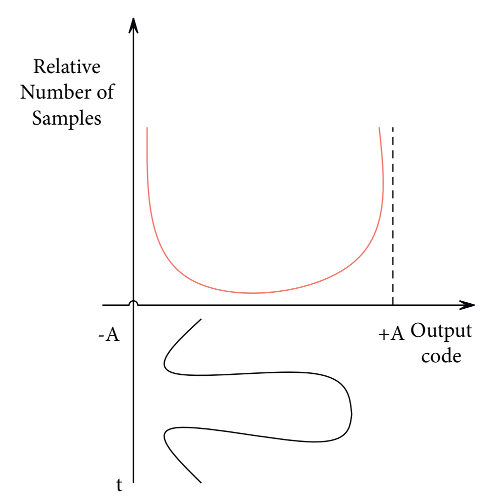

Figure 7: Histogram of ideal code density for sine wave input.

$$F_t(t) = \begin{cases} \dfrac{1}{T}, 0 \le t \ge T, \\ 0, otherwise, \end{cases} \tag{19}$$

where $F_t(t)$ is the probability density function of t, and V_{IN} is the function of the random variable t. From this, the probability density function of the sine wave V_{IN} can be obtained:

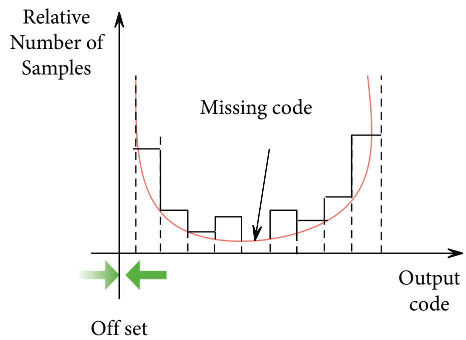

Figure 8: Density histogram of actual code of sine wave input.

$$P(V_{IN}) = \left|\frac{d}{d_{V_{IN}}} g^{-1}(V_{IN})\right| f_t(V_{IN}) = \frac{1}{\pi\sqrt{A^2 - V_{IN}^2}}. \tag{20}$$

Its distribution is shown in the figure. We integrate the probability density function of formula (14) and assume that the integration interval is $[V_a, V_b]$. Then, there is:

$$\begin{aligned} P(V_a, V_b) &= \int_{V_a}^{V_b} \frac{1}{\pi\sqrt{A^2 - V_{IN}^2}} dV \\ &= \frac{1}{\pi}\left\{\sin^{-1}\left[\frac{V_b}{A}\right] - \sin^{-1}\left[\frac{V_a}{A}\right]\right\}. \end{aligned} \tag{21}$$

$P(V_a, V_b)$ is the sampling probability in the $[V_a, V_b]$ voltage interval. We set $V_b - V_a = 1$ to get the discrete probability distribution function z:

$$P(i, A) = \frac{1}{\pi}\left\{\sin^{-1}\left[\left(\frac{2i - 2^n - 1}{2^n}\right)\frac{V_{ref}}{A}\right] - \sin^{-1}\left[\left(\frac{2i - 2^n - 3}{2^n}\right)\frac{V_{ref}}{A}\right]\right\}, \tag{22}$$

$P(i, A)$ is the probability that code i appears in the code box Bin $[i]$. V_{ref} is the full-scale voltage of the AD conversion circuit.

If the sine wave of the channel has a DC offset, which is set to V, there is $V_{IN} = V_0 + A\sin(\omega t)$, the probability density function is:

$$P(V) = \frac{1}{\pi\sqrt{A^2 - (V - V_0)^2}}. \tag{23}$$

Similarly, the probability density distribution function can be obtained:

$$\begin{aligned} P(V_a, V_b) &= \int_{V^a}^{V^b} \frac{1}{\pi\sqrt{A^2 - (V - V_0)^2}} dV \\ &= \frac{1}{\pi}\left\{\sin^{-1}\left[\frac{V_b - V_0}{A}\right] - \sin^{-1}\left[\frac{V_a - V_0}{A}\right]\right\}. \end{aligned} \tag{24}$$

We set $V_b - V_a = 1$, and in the same way, the discrete probability distribution function can be obtained:

$$P(i, A, V_0) = \frac{1}{\pi}\left\{\sin^{-1}\left[\left(\frac{2i - 2^n - 1 - 2V_0}{2^n}\right)\frac{V_{ref}}{A}\right] - \sin^{-1}\left[\left(\frac{2i - 2^n - 3 - 2V_0}{2^n}\right)\frac{V_{ref}}{A}\right]\right\}. \tag{25}$$

Derivation of calculation formula for ADC conventional dynamic conversion characteristic parameter test.

We set the code box corresponding to the output code i of the ADC to be $H[i]$, there are:

$$CH[i] = \sum_{j=0}^{i} H[i], \tag{26}$$

and it is an offset error.

If the ADC offset is zero, the sine wave histogram is symmetrical with respect to the midpoint, that is, the sum of the bin widths on both sides of the midpoint is equal. If the ADC has an offset V_d, the balance will be broken, and the sum of the widths of the code boxes on both sides of the middle point will be different. We set:

$$N_n = \sum_{i=1}^{2^{n-1}} H[i], N_p \sum_{i=2^{n-1}+1}^{2^n} H[i]. \tag{27}$$

We set P_d to be the probability that the randomly sampled voltage is positive, that is, the sampled voltage is within $(0, A + V_d)$. Pn is the probability that the randomly sampled voltage is negative, that is, the sampled voltage is within $(-A + V_d, 0)$. Then, there is formula (18) to get:

$$P_p = \frac{1}{\pi}\left\{\sin^{-1}(1) + \sin^{-1}\left(\frac{V_d}{A}\right)\right\} = \frac{1}{2} + \frac{1}{\pi}\sin^{-1}\left(\frac{V_d}{A}\right). \tag{28}$$

The entire sampling is an inevitable event, that is, $P_p + P_n = 1$. From this, we get:

$$P_n = \frac{1}{2} - \frac{1}{\pi}\sin^{-1}\left(\frac{V_d}{A}\right). \tag{29}$$

There are two formulas (22) and (23), we can solve:

$$V_d = A\frac{\pi}{2}\sin\left(P_p - P_n\right). \tag{30}$$

According to probability theory, P_p and P_n can be approximated by N_n/N_t and N_p/N_t, N_t is the total number of samples, and the estimated value of the offset V_d can be obtained:

$$V_d = A\frac{\pi}{2}\sin\frac{N_p - N_n}{N_p + N_n}. \tag{31}$$

In general, the offset V_d is small compared to the sine wave amplitude A, so the above formula can be further approximated as:

$$V_d = A\frac{\pi}{2}\frac{N_p - N_n}{N_p + N_n}. \tag{32}$$

The differential nonlinear DNL theoretical formula is the ratio of the actual probability of the code to the ideal probability minus 1, that is:

$$DNL = \frac{P_A(n)}{P_I(n)} - 1. \tag{33}$$

Among them, $P_A(n)$ is the actual probability of the occurrence of the nth code of the ADC, and $P_I(n)$ is the ideal probability of the occurrence of the nth code. In (18), $H[i]/N_t$ is used to approximate $P\,(V_a.\,V_b)$, and the estimated value $\widehat{V}_b$ of V_b can be calculated. Because the offset voltage does not affect the integral and differential nonlinearity, it can be solved by formula (18):

It is obtained by the formula:

$$\begin{aligned}\widehat{V}_b^2 &= V_a\cos\left(\frac{\pi H[i]}{N_t}\right)(2V_a)\widehat{V}_b\\ &- A^2\left(1-\cos^2\left(\frac{\pi H[i]}{N_t}\right)\right) + V_a^2 = 0.\end{aligned} \tag{34}$$

$$\cos\left(\sin^{-1}\frac{V}{A}\right) = \frac{\sqrt{A^2 - V^2}}{A}. \tag{35}$$

We solve formula (18), and we can get:

$$\begin{aligned}&\widehat{V}_b^2 - \left(2V_a\cos\left(\frac{\pi H[i]}{N_t}\right)\right)\widehat{V}_b - A^2\left(1-\cos^2\left(\frac{\pi H[i]}{N_t}\right)\right)\\ &+ V_a^2 = 0.\end{aligned} \tag{36}$$

Only positive roots can be taken to solve the equation, and we can get:

$$\widehat{V}_b^2 = V_a\cos\left(\frac{\pi H[i]}{N_t}\right) + \sin\left(\frac{\pi H[i]}{N_t}\right)\sqrt{A^2 - V_{i-1}^2}. \tag{37}$$

The discrete relation $V_b - V_a = 1$ is brought in, then we have:

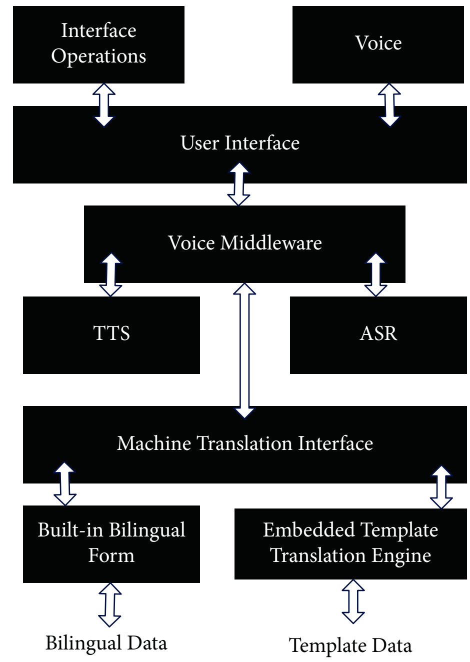

Figure 9: Intelligent computer-aided translation system.

$$\widehat{V}_t = V_{i-1}\cos\left(\frac{\pi H[i]}{N_t}\right) + \sin\left(\frac{\pi H[i]}{N_t}\right)\sqrt{A^2 - V_{i-1}^2}. \tag{38}$$

The recursive formula does not produce a cumulative error. Therefore, $\widehat{V}_i$ can be calculated from the boundary condition $V_1 = -A$ and the cumulative histogram CH $[i]$:

$$\widehat{V}_i = -A\cos\left(\frac{\pi CH[i]}{N_t}\right). \tag{39}$$

In the equation, A is a linear unknown, which can be normalized, namely:

$$\overline{V}_i = -\cos\left(\frac{\pi CH[i]}{N_t}\right). \tag{40}$$

From this, the calculation formulas of differential nonlinearity (DNL) and integral nonlinearity (INL) can be obtained:

$$\begin{aligned}DHL &= \frac{\overline{V}[i+1] - \overline{V}[i]}{1LSB},\\ INL &= \frac{\overline{V}[i] - \overline{V}[1]}{1LSB} - (i-1).\end{aligned} \tag{41}$$

3. System Construct and Test

Based on the algorithm of the second part, the intelligent computer-aided translation system constructed in this study is shown in Figure 9.

The dCFT translation system adopts the sine wave code density test, and the ratio of the ADC sampling frequency and the input sine wave frequency is irrelevant to meet the irrelevant condition. In order to achieve a 95% confidence

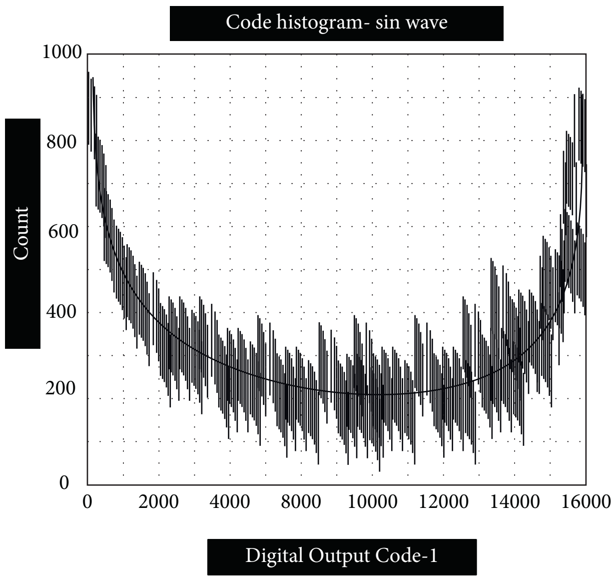

Figure 10: Histogram of ADC full-scale bin (bathtub curve).

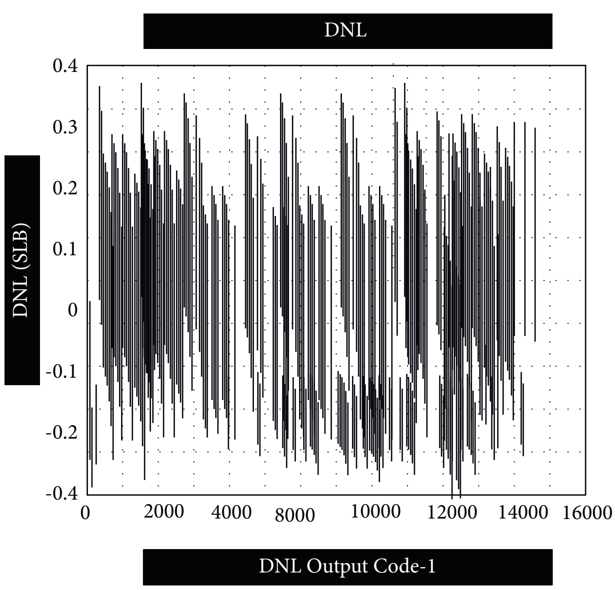

Figure 11: ADC DNL differential phenanthrene linear curve (95%). Therefore, at 95% confidence, $ADCDNL \approx -0.3 + 0.3\,(LSB)$.

rate, the 14-bit ADC needs to be tested more than 10,000,000 times. The sine wave data are drawn by Matlab, and the statistical histogram of each code box of the ADC is shown in Figure 10:

The ADC dynamic DNL curve can be calculated by bringing the code box statistical histogram into formula (18), as shown in Figure 11:

On the basis of the above research, the system proposed in this study is applied to translation teaching to explore its teaching effect. The results of the expert evaluation are shown in Table 1.

Table 1: The application effect of computer-assisted translation technology in translation teaching.

Num	Teaching effect	Num	Teaching effect
1	79.37	18	85.12
2	82.43	19	82.34
3	81.83	20	84.67
4	79.91	21	81.56
5	79.33	22	84.69
6	83.36	23	83.97
7	79.76	24	80.06
8	83.24	25	84.72
9	83.87	26	84.26
10	81.13	27	81.31
11	80.20	28	80.01
12	83.04	29	83.06
13	79.61	30	83.64
14	85.88	31	83.52
15	83.61	32	84.98
16	81.96	33	84.75
17	81.29	34	85.27

Through teaching evaluation research, it is verified that the application effect of computer-assisted translation technology in translation teaching is very good.

4. Conclusion

With the continuous development of computer technology, the degree of human dependence on computers is also rising rapidly. Therefore, how to solve the communication between people and computers has become the focus of the scientific community, which is also known as "intelligent human–computer interaction" technology. Among them, the most striking is undoubtedly the communication with the computer through language. The system proposed in this study is a multi-language intelligent translation terminal software system realized by using advanced technologies such as speech recognition, machine translation, speech synthesis, and an embedded multi-language service system framework. Moreover, this study combines computer-assisted translation technology to construct a translation teaching system to improve the quality of translation teaching in colleges and universities. In addition, this study verifies that the application of computer-assisted translation technology in translation teaching is very good through teaching evaluation research.

Data Availability

The labeled dataset used to support the findings of this study is available from the corresponding author upon request.

Conflicts of Interest

The authors declare that they have no conflicts of interest.

Acknowledgments

The research was supported by The Construction and Practice of Digital Resource of Moral Education in College English based on Blended-learning (Teaching Reform and Research Project of College English by Hebei Education Department).

References

[1] M. Rodríguez-Castro, "An integrated curricular design for computer-assisted translation tools: developing technical expertise," *The Interpreter and Translator Trainer*, vol. 12, no. 4, pp. 355–374, 2018.

[2] K. Taivalkoski-Shilov, "Ethical issues regarding machine (-assisted) translation of literary texts," *Perspectives*, vol. 27, no. 5, pp. 689–703, 2019.

[3] R. Shadiev, A. Sun, and Y. M. Huang, "A study of the facilitation of cross-cultural understanding and intercultural sensitivity using speech-enabled language translation technology," *British Journal of Educational Technology*, vol. 50, no. 3, pp. 1415–1433, 2019.

[4] R. Shadiev and Y. M. Huang, "Investigating student attention, meditation, cognitive load, and satisfaction during lectures in a foreign language supported by speech-enabled language translation," *Computer Assisted Language Learning*, vol. 33, no. 3, pp. 301–326, 2020.

[5] A. Tambusai, "Error analysis of instagram machine translation in Indonesia into English," *AFoSJ-LAS (All Fields of Science Journal Liaison Academia and Society)*, vol. 2, no. 2, pp. 261–271, 2022.

[6] F. Yasmin, "Challenges to computer assisted language teaching at university level," *INTERNATIONAL JOURNAL OF LANGUAGE & LITERATURE*, vol. 6, no. 2, pp. 86–93, 2018.

[7] S. M. Lee and N. Briggs, "Effects of using machine translation to mediate the revision process of Korean university students' academic writing," *ReCALL*, vol. 33, no. 1, pp. 18–33, 2021.

[8] R. Hussain, A. Lalande, C. Guigou, and A. Bozorg-Grayeli, "Contribution of augmented reality to minimally invasive computer-assisted cranial base surgery," *IEEE Journal of Biomedical and Health Informatics*, vol. 24, no. 7, pp. 2093–2106, 2020.

[9] D. Tafazoli, M. Gómez Parra, and H. Abril, "A cross-cultural study on the attitudes of English language students towards Computer-Assisted Language Learning," *Teaching English with Technology*, vol. 18, no. 2, pp. 34–68, 2018.

[10] P. Hendikawati, M. Z. Zahid, and R. Arifudin, "Android-based computer assisted instruction development as a learning resource for supporting self-regulated learning," *International Journal of Instruction*, vol. 12, no. 3, pp. 389–404, 2019.

[11] D. Zou, Y. Huang, H. Xie, D. Sa Zou, Y. Huang, and H. Xie, "Digital game-based vocabulary learning: where are we and where are we going?" *Computer Assisted Language Learning*, vol. 34, no. 5-6, pp. 751–777, 2021.

[12] R. Knowles, M. Sanchez-Torron, and P. Koehn, "A user study of neural interactive translation prediction," *Machine Translation*, vol. 33, no. 1-2, pp. 135–154, 2019.

[13] B. Raji, "Significance and challenges of computer assisted education programs in the UAE: a case study of higher learning and vocational education," *Education and Information Technologies*, vol. 24, no. 1, pp. 153–164, 2019.

[14] J. Kubicek, F. Tomanec, M. Cerny, D. Vilimek, M. Kalova, and D. Oczka, "Recent trends, technical concepts and components of computer-assisted orthopedic surgery systems: a comprehensive review," *Sensors*, vol. 19, no. 23, p. 5199, 2019.

[15] C. A. Lenkaitis, "Technology as a mediating tool: videoconferencing, L2 learning, and learner autonomy," *Computer Assisted Language Learning*, vol. 33, no. 5-6, pp. 483–509, 2020.

[16] A. D'Urso, V. Agnus, M. Barberio et al., "Computer-assisted quantification and visualization of bowel perfusion using fluorescence-based enhanced reality in left-sided colonic resections," *Surgical Endoscopy*, vol. 35, no. 8, pp. 4321–4331, 2021.